

CFD MODELING OF PARTICULATES MOTION IN GAS PIPELINES

Vahid Abdolkarimi, Saeed Hassan Boroojerdi

Development and Engineering Department, Research Institute of Petroleum Industry,
Tehran, 1485733111, Iran, Abdolkarimiv@RIPI.ir

Received June 11, 2013, Accepted September 20, 2013

Abstract

In this study the computational fluid dynamics modeling of solid particles hydrodynamic in gas flow inside a gas pipeline, with 10 meters length and 56 inches diameter, at different gas velocities is considered based on Eulerian formulation for multiphase flows to find out the fluidization pattern of solid particles. Then, the computational modeling based on Lagrangian framework for diluted solid-gas flow through 90° gas pipeline bend is carried out to discover the effect of particles size distribution on particles flow pattern and their trajectory. Particles size distribution has been obtained experimentally by measuring the size of solid particles that are flowing through the gas pipelines of Aghajari gas booster station. The pipeline bend under study has a pipe diameter of 56 inches and ratios of the bend radius of the curvature to the pipeline diameter of 1.5. For the validation of computational model, at first the computational modeling is performed for a published experimental solid-gas flow data. The computational results include radial gas velocity and radial particle velocity profiles on planes which are at different angles through the bend. The comparison between predicted numerical results with similar experimental data proves that the predictions of computational model are acceptable.

Keywords: CFD; Eulerian formulation; Lagrangian framework; solid-gas flow.

1. Introduction

In the oil and gas industry, Black Powder (BP) is the brief name that is used to describe the black materials found inside the most of gas pipelines worldwide. Black powder can be found in several forms, such as wet with a tar-like appearance or dry in the form of a very fine powder [1-5]. It is composed of different forms of iron sulfide (FeS), iron oxides (Fe₃O₄, FeOOH) and iron carbonate (FeCO₃), mechanically mixed or chemically combined with any number of contaminants, such as salts, sand, liquid hydrocarbons, metal debris [2]. Once BP exists and is moving with the flow, it can represent a serious threat to the integrity of the gas pipelines by eroding compressor components and pipeline control valves, plugging metering instrumentation and filters, and reducing the accuracy of the in-line inspection. Also, BP could have major adverse effects on customers by contaminating the customers' sales gas supply leading to interruptions of the customers' operations and/or poor quality of products in which the sales gas is used as feedstock [3].

The required fluid velocity has been determined [6-7] to entrain and carry away BP in liquid and gas pipelines, respectively. These two studies concluded that the velocity required to move BP particles in gas pipelines is independent of particle size and ranges from 10.4 ft per second (fps) to 13.6 fps for 8" and 30" pipelines, respectively. In liquid pipelines, the water velocity required depends on the equivalent particle size, up to a size of about 5.0 millimeters, after which it depends only on the pipe diameter.

The effect of the drag coefficient and inlet conditions (inlet velocity profile) of solid particles on the particle tracks calculations in vertical and horizontal ducts are studied [8] using the commercial computational fluid dynamics (CFDs) package, CFX 4.4. They found that the drag coefficient needs to be reduced by as much as 35% of the standard value to achieve good agreement with the corresponding experimental data in case of a vertical channel flow. On the other hand, for a horizontal channel flow it needs to be reduced only 20% to achieve similar

agreement. Regarding the velocity inlet conditions, it was reported [8] that the vertical turbulent flow seems to be insensitive to the inlet conditions while for a horizontal flow it is found to be strongly dependent on inlet conditions.

CFD simulations have been performed [9] on a diluted particulate turbulent flow in a 90° duct bend with a radius of curvature equal to a 1.5 duct (225 mm) hydraulic diameter. As in previous work [8], simulations were performed using CFX 4.4, using the differential Reynolds stress model (DRSM) with fully developed inlet conditions to solve the turbulent flow in the bend, and also used the same test facility to produce the experimental data used in validating the simulations. In another work [10] the author used different solid size distributions rather than a single uniform particle size, and also made use of a modified shear-slip lift force formula, which is consistent with experimental data for. From these studies [8-9], it was concluded that the DRSM did not capture the correct pressure gradient effects within the bend. Also, it was found that even the finer particles (66 micron) experienced a gas-solid segregation due to the centrifugal effect. This segregation was characterized by a local drop in particle concentration near the inner wall and was well reflected in predictions where the averaged velocity profiles discontinued in the locality. The experimental part of the study [10] is reported in more detail [11].

Solid particulates that are flowing inside gas pipelines (BP) of Aghajari gas booster station have been analyzed. CFD modeling of particles fluidization which is based on Eulerian formulation is carried out using averaged particles size. For evaluating the effect of particles size on particles motion and fluidization, CFD modeling based on Lagrangian framework is performed for a 90° gas pipeline bend. Particles size distribution is considered in the modeling by Rosin-Rammler distribution function.

2. Geometry and Flow Conditions

There are two kinds of geometry of gas pipelines under consideration: (1) A 10 meters long pipe with 56 inches diameter which is used to evaluate the fluidization pattern of averaged size particles at different gas inlet velocities. The relevant CFD model is based on Eulerian framework. (2) A 90° angled bend with ratios of the bend radius of the curvature to the pipeline diameter of 1.5 which is used for detailed modeling of particles motion which is associated with particles size distribution. This CFD modeling is performed based on Lagrangian framework.

Particles size distribution has been obtained experimentally by measuring the size and the relevant mass of solid particles that is flowing through the gas pipelines of Aghajari gas booster station by the use of woven wire test sieve (WWTS). Particles size and mass distribution is given in table1.

Particles are collected at the sampling point of 56 inches diameter pipe which is the primary inlet pipeline to Aghajari gas station. After 500 hours, 300 kg of particles was obtained that indicates the mass flow rate of particles is 0.6 kg/hr. The measured density of particles is 2303 kg/m³. The stream of main inlet pipe is distributed between seven compressors which one of them works at the normal condition. Therefore, the gas flow rate at normal condition which is used for modeling purpose is 600 SMMCF/H. The pressure and temperature of supplied gas in main inlet pipe are 80 barg and 40 °C respectively.

Table1. Particles size and mass distribution

Sieve Disk.NO	Particles size (μm)	Particles mass (gr)	(Wt%)
6	d>3350	14.73	7
8	3350>d>2360	17.45	8.2
12	2360>d>1700	15.6	7.4
16	1700>d>1180	19.4	9.2
20	1180>d>850	41	19.4
30	850>d>600	20.94	9.9
40	600>d>425	15.88	7.5
50	425>d>300	13.18	6.1
70	300>d>212	12.72	6.0
100	212>d>150	28.42	13.5
200	150>d>125	12.42	5.8

3. Mathematical Model

The commercial CFD software FLUENT 6.3 is used to solve the Reynolds Averaged Navier-Stokes (RANS) equations. For evaluating the effect of gas inlet velocity on particles fluidization pattern the Eulerian framework for solid-gas flow modeling is used. In this model both phases are considered as continuous phases that are penetrating each other. The effect of continuous gas phase on particles is determined by interphase drag force. The contribution of each phase in continuity and momentum equations are specified by the volume fraction of each phase. The closure equations for solid phase are obtained from the kinetic theory of granular flow. The continuity equation for each phase is:

$$\frac{\partial(\alpha_k \rho_k)}{\partial t} + \nabla \cdot (\alpha_k \rho_k \vec{U}_k) = 0 \quad (1)$$

where \vec{U}_k is the velocity and α_k is the volume fraction of each phase.

Momentum balance equation for solid phase is:

$$\frac{\partial}{\partial t} (\alpha_s \rho_s \vec{u}_s) + \nabla \cdot (\alpha_s \rho_s \vec{u}_s \vec{u}_s) = -\alpha_s \nabla P - \nabla P_s + \nabla \cdot \overline{\overline{\tau}}_s + \alpha_s \rho_s g + \sum_{g=1}^n \beta_{gs} (\vec{u}_g - \vec{u}_s) \quad (2)$$

The solid phase shear stress $\overline{\overline{\tau}}_s$ is computed as follows:

$$\alpha_s \overline{\overline{\tau}}_s = -P_s \overline{\overline{I}} + \alpha_s \mu_s (\nabla u_s + (\nabla u_s)^T) + \alpha_s (\lambda_s - 2/3 \mu_s) \nabla u_s \quad (3)$$

where P_s is solid pressure, μ_s is solid shear viscosity and λ_s is solid bulk viscosity.

Solid pressure is computed by Lun's equation:

$$P_s = \alpha_s \rho_s \Theta_s + 2\rho_s (1 + e_{ss}) \alpha_s^2 g_{0,ss} \Theta_s \quad (4)$$

where e_{ss} is the coefficient of restitution for particle collisions with default value of 0.9 that indicates the particle's collision is close to elastic collision, $g_{0,ss}$ is the radial distribution function, and Θ_s is the granular temperature. The granular temperature is proportional to the kinetic energy of the fluctuating particle motion. The conservation equation for granular temperature is:

$$\frac{3}{2} \left[\frac{\partial}{\partial t} (\rho_s \alpha_s \Theta_s) + \nabla \cdot (\rho_s \alpha_s \Theta_s v_s) \right] = (-P_s \overline{\overline{I}} + \overline{\overline{\tau}}_s) : \nabla v_s - \nabla \cdot (k_{\theta_s} \nabla \Theta_s) - \gamma_{\theta_s} \quad (5)$$

The term $\nabla \cdot (k_{\theta_s} \nabla \Theta_s)$ describing the diffusive flux of granular energy. The term γ_{θ_s} , represents the rate of energy dissipation within the solid phase due to collisions between particles.

$$\gamma_{\theta_s} = \frac{12(1 - e_{ss}^2) g_{0,ss}}{d_s \sqrt{\pi}} \alpha_s^2 \rho_s \Theta_s^{3/2} \quad (6)$$

Lun's equation for $g_{0,ss}$ is:

$$g_{0,ss} = \left[1 - \left(\frac{\alpha_s}{\alpha_{s,\max}} \right) \right]^{-2.5 \alpha_{s,\max}} \quad (7)$$

Solid shear viscosity is:

$$\mu_s = \mu_{s,col} + \mu_{s,kin} + \mu_{s,fric} \quad (8)$$

The frictional part of solid viscosity is only important when the solid volume fraction become close to solid packing limit ($\alpha_{s,max}$).

The contribution of collision in solid viscosity is:

$$\mu_{s,col} = \frac{4}{5} \alpha_s \rho_s d_s g_{0,ss} (1 + e_{ss}) \sqrt{\frac{\Theta_s}{\pi}} \quad (9)$$

The kinetic viscosity is computed in terms of Gidaspow's equation:

$$\mu_{s,kin} = \frac{10 d_s \rho_s \sqrt{\Theta_s \pi}}{96 \alpha_s (1 + e_{ss}) g_{0,ss}} \left[1 + \frac{4}{5} g_{0,ss} \alpha_s (1 + e_{ss}) \right]^2 \quad (10)$$

The bulk viscosity of solid phase is given by Lun's equation:

$$\lambda_s = 4/3 \alpha_s \rho_s d_p g_{0,ss} (1 + e_{ss}) \sqrt{\frac{\Theta_s}{\pi}} \quad (11)$$

The solids bulk viscosity accounts for the resistance of the granular particles to compression and expansion.

The interphase drag coefficient (β_{gs}) is calculated according to Gidaspow's equation:

$$\beta_{Ergun} = 150 \frac{\alpha_s^2 \mu_g}{\alpha_g d_s^2} + 1.75 \frac{\alpha_s \rho_g}{d_s} |v - u| \quad \alpha_g < 0.8 \quad (12)$$

$$\beta_{Wen-Yu} = 3/4 C_D \frac{\alpha_s \alpha_g \rho_g}{d_s} |v - u| \alpha_g^{-2.65}, \alpha_g \geq 0.8 \quad (13)$$

The geometry which is used for evaluating fluidization pattern is a 10 meters long pipe with 56 inches diameter. It is assumed that particles are settled in the pipe and the effect of gas flow with different inlet velocities on particles bed is considered.

4. Lagrangian framework for modeling solid-gas flow

For considering the effect of particles size distribution on particles motion and particles trajectory the Lagrangian framework for modeling diluted solid-gas flow is used. Flowing particles in the main gas pipeline of Aghajari station has been gathered and analyzed by woven wire test sieve to determine the size and mass distribution of particles (table1). The Rosin-Rammler distribution function is used to specify the fraction of particles with specific sizes. The mass fraction of particles of diameter greater than d is given by:

$$Y_d = e^{-\left(\frac{d}{\bar{d}}\right)^n} \quad (14)$$

where \bar{d} is the size constant and n is the size distribution parameter.

The trajectory of a discrete phase particle is predicted by integrating the force balance on the particle. This force balance equates the particle inertia with the forces acting on the particle, and can be written (for the x direction in Cartesian coordinates) as:

$$\frac{du_p}{dt} = F_D + \frac{g_x (\rho_p - \rho)}{\rho_p} \quad (15)$$

The drag force imposed on the droplet is given by equation (16):

$$F_D = \frac{18 \mu C_D \text{Re}}{\rho_p d_p^2} (u - u_p) \quad (16)$$

$$C_D = a_1 + \frac{a_2}{\text{Re}} + \frac{a_3}{\text{Re}^2} \quad (17)$$

$$\text{Re} = \frac{\rho d_p |u - u_p|}{\mu} \quad (18)$$

The particles path is computed by integrating of equation (19):

$$\frac{dx}{dt} = u_p \quad (19)$$

The dispersion of particles due to gas phase turbulence is accounted by The Discrete Random Walk Model.

Due to the high gas velocity (33m/s) and high strain rate of fluid near the pipe wall the Realizable k-e model is used for modeling gas phase turbulence.

$$\frac{\partial}{\partial t}(\rho_g k_g) + \nabla \cdot (\rho_g k_g \vec{U}_g) = \nabla \cdot \left[\left(\mu + \frac{\mu_{t,g}}{\sigma_k} \right) \nabla k_g \right] + G_{k,g} - \rho_g \varepsilon_g \quad (20)$$

$$\frac{\partial}{\partial t}(\rho_g \varepsilon_g) + \nabla \cdot (\rho_g \varepsilon_g \vec{U}_g) = \nabla \cdot \left[\left(\mu + \frac{\mu_{t,g}}{\sigma_k} \right) \nabla \varepsilon_g \right] + \varepsilon_g \left(-\rho_g C_2 \frac{\varepsilon_g}{k_g + \sqrt{\nu_g \varepsilon_g}} \right) \quad (21)$$

where σ_ε , σ_k are turbulent Prandtl number and $\mu_{t,g}$ is turbulent viscosity. k_g and ε_g are turbulent kinetic energy and dissipation rate respectively.

$$\mu_t = \rho C_\mu \frac{k^2}{\varepsilon} \quad (22)$$

$$C_\mu = \frac{1}{A_0 + A_S \frac{kU^*}{\varepsilon}} \quad (23)$$

$$U^* = \sqrt{S_{ij} S_{ij}} \quad (24)$$

$$A_0 = 4.04, A_S = \sqrt{6} \cos \phi \quad (25)$$

$$\phi = \frac{1}{3} \cos^{-1}(\sqrt{6}W), W = \frac{S_{ij} S_{jk} S_{ki}}{\tilde{S}^3}, \tilde{S} = \sqrt{S_{ij} S_{ij}}, S_{ij} = \frac{1}{2} \left(\frac{\partial u_j}{\partial x_i} + \frac{\partial u_i}{\partial x_j} \right) \quad (26)$$

The geometry that is used for modeling particulates motion consists of a 90° angled bend with ratios of the bend radius of the curvature to the pipeline diameter of 1.5.

5. Validation of the Mathematical Model

The published experimental data [11] was used to validate the mathematical model based on Lagrangian framework for modeling a diluted gas-solid flow through a curved 90° duct bend. The curved bend is squared-section (15 cm x 15 cm) and has a radius of curvature, R of 1.5 times the duct hydraulic diameter, D , (22.5 cm). Gas phase measurements were obtained using a Laser Doppler Anemometer (LDA) at a bulk gas velocity, V_B , of 10 m/s in the absence of solid phase. The solid phase, which is glass spheres with an average diameter of 66 μm , was released into the flow from a fluidized bed. The solids/ gas mass loading ratio reached is well below 1%, so as to setup a diluted gas-solid flow regime. The radial velocity profiles of gas and particles are compared with similar measurement data that is obtained from different cross sectional planes through the squared bend (figure 1).

In figure 2 the predicted radial distribution of gas velocity is compared with experimental data.

Radial distance, r , is computed by the equation (27):

$$r = R + D/2 - r^* \quad (27)$$

where R is the curve radius of duct, D , is the hydraulic diameter of duct and r^* , is the distance of any point on a special cross sectional plane, from the origin.

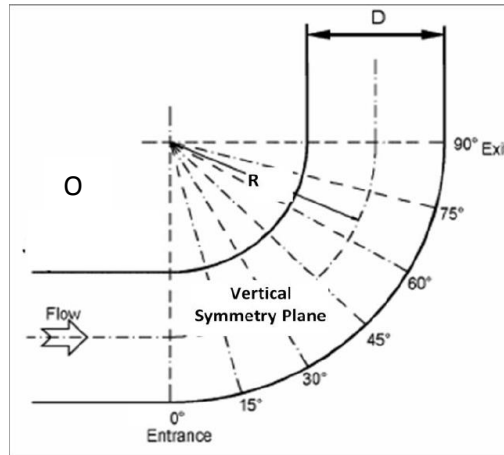


Figure 1. Cross sectional planes through bend [12]

As it is shown in figure 2 by increasing the cross sectional planes angle the more conformity between predicted profiles and measured profiles achieves. This can be due to decreasing the radial component of gas velocity.

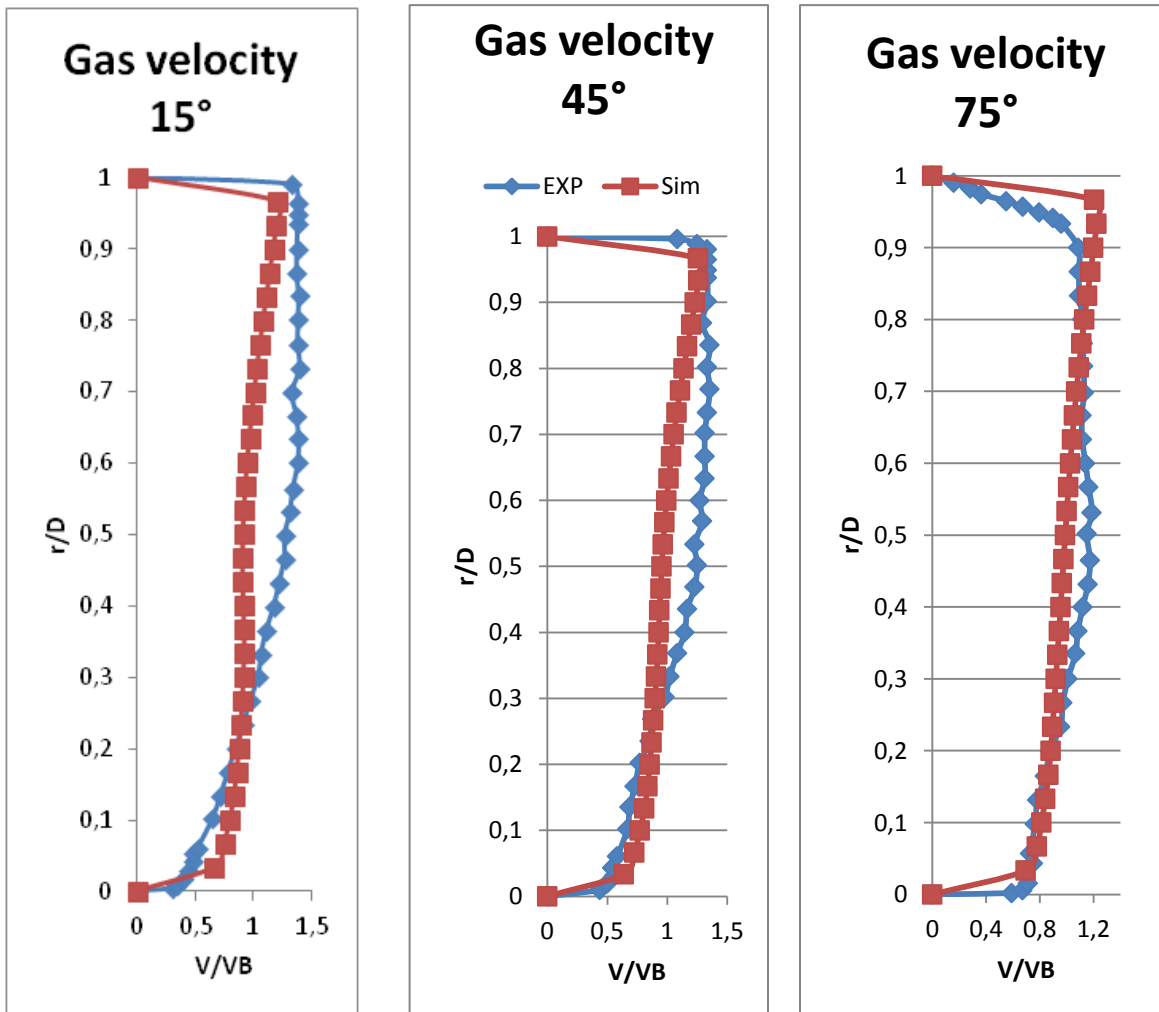


Figure 2. Radial distribution of gas velocity over cross sectional planes

In figure 3 the predicted radial distribution of particles velocity is compared with experimental measurements. As can be seen, predicted results show that particles velocity profile do not continue to inner wall. This is due to the radial component of gas velocity that leads to moving particles toward the outer wall of the bend. Figure4 shows the radial velocity vectors of gas inside the bend.

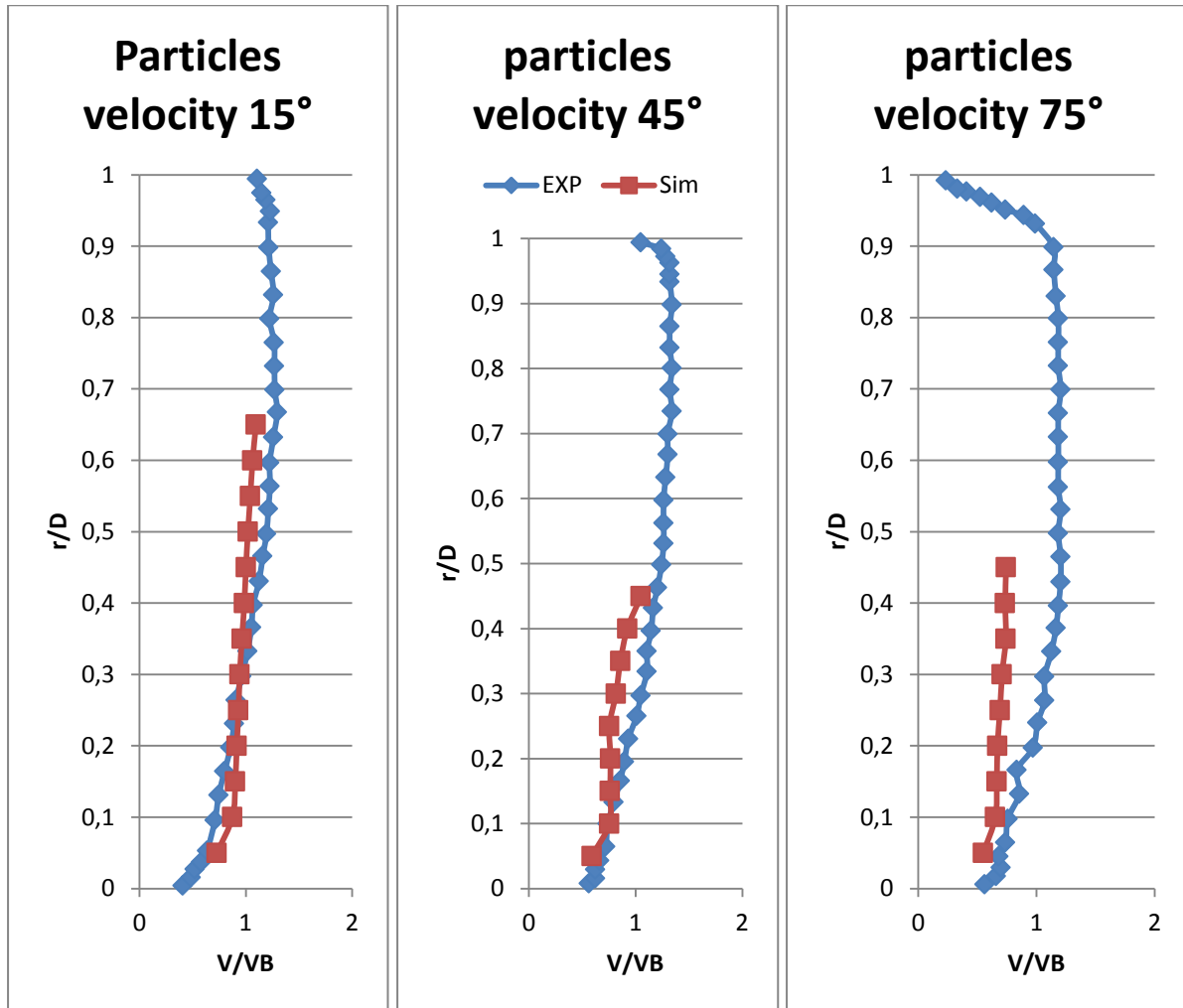


Figure 3. Radial distribution of particles velocity over cross sectional planes

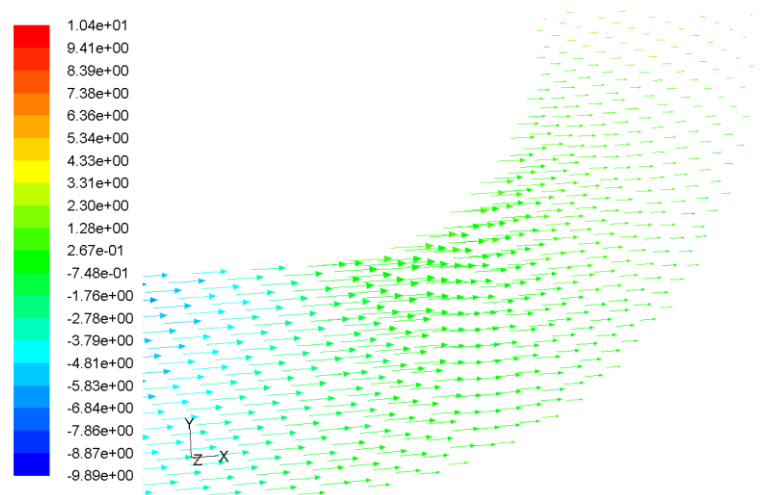


Figure 4. Radial velocity vectors of gas

6. Results and Discussion

Solid particles fluidization in gas flow inside a gas pipeline, with 10 meters length and 56 inches diameter, at different gas velocities was considered based on Eulerian formulation. It is supposed that at the first, solid particles settle on the down wall of the pipe (figure5) and the gas flows over them. Figure6 shows the fluidization pattern of particles at different gas inlet velocities after sufficient elapsed time from onset of gas flow. At the inlet gas velocity of 0.5 m/s the solid particles become fluidized. For gas velocity above 0.5 m/s particles are moved by the gas flow. The more gas bulk velocity, the more speed at which particles are moved. As can be seen from figure6 at gas inlet velocity of 1 m/s after 134s, the most of the particles are moved out of the pipe. By increasing the gas inlet velocity we can see if there is not any source of solid particles in the pipe, the whole of particles are moved out completely and there will not remain any fluidized particle inside the pipe. At the minimum gas flow rate, the gas velocity is 33 m/s therefore it can be concluded that without any particle sources inside the pipe after a few minutes there is no particle in the pipe.

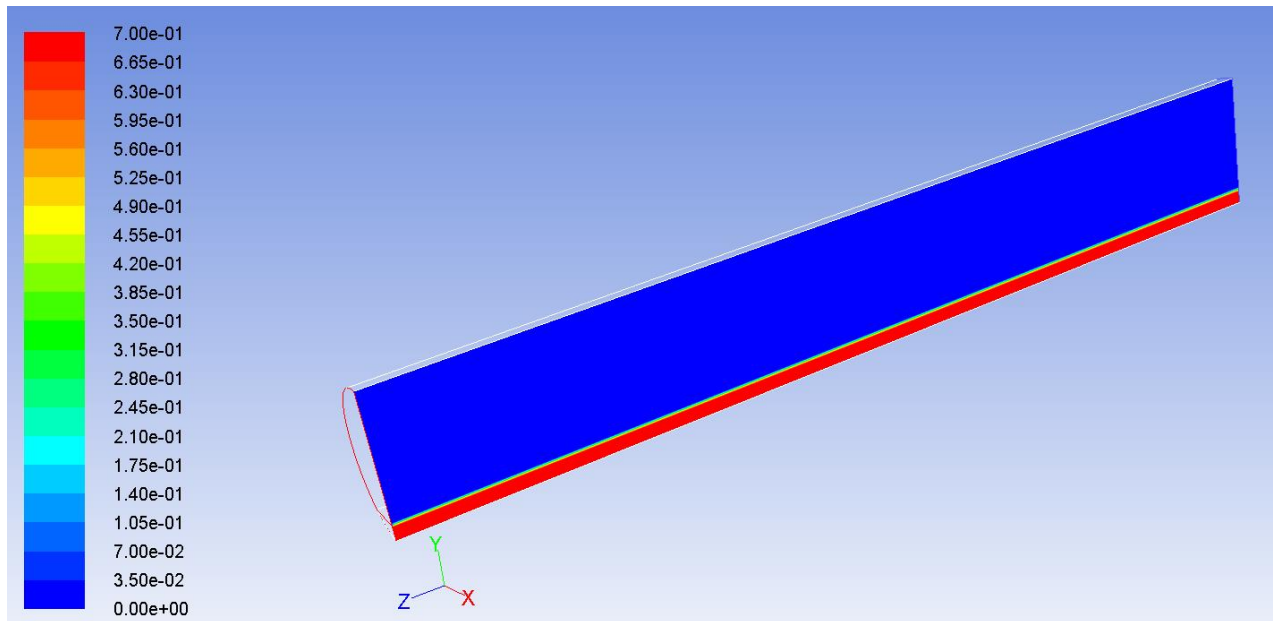
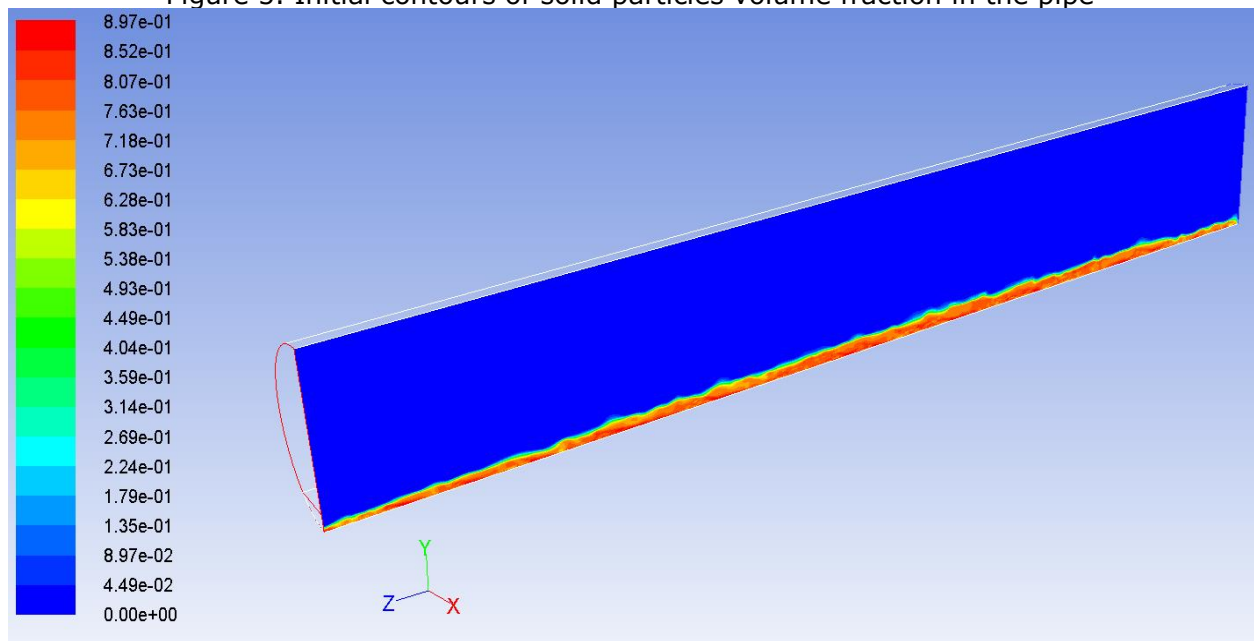
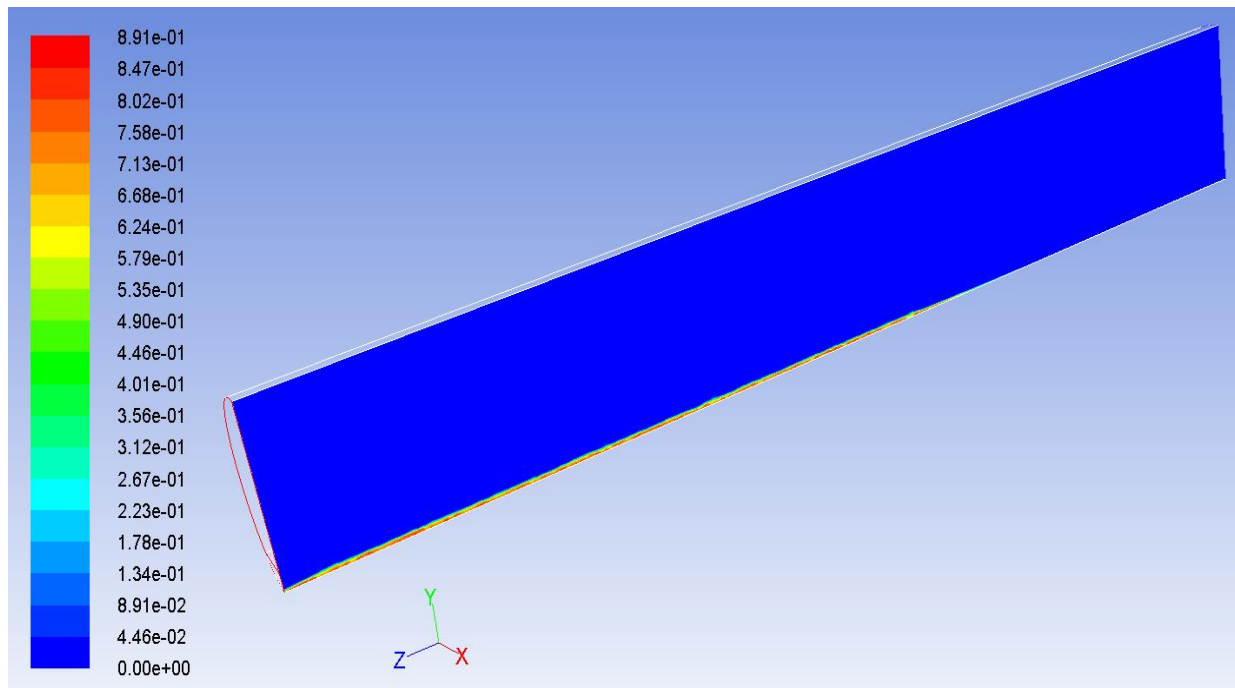


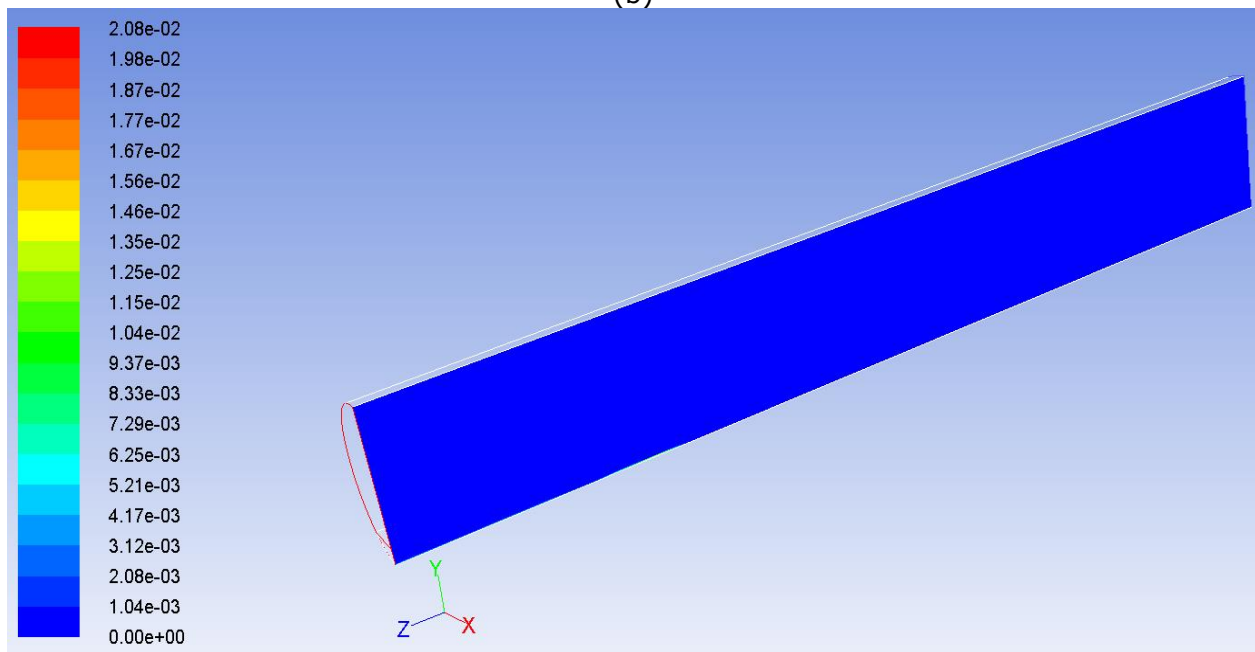
Figure 5. Initial contours of solid particles volume fraction in the pipe



(a)



(b)



(c)

Figure 6. The contours of particles volume fraction (a) at gas velocity of 0.5 m/s after 140s (b) at gas velocity of 1 m/s after 134s (c) at gas velocity of 6 m/s after 42s

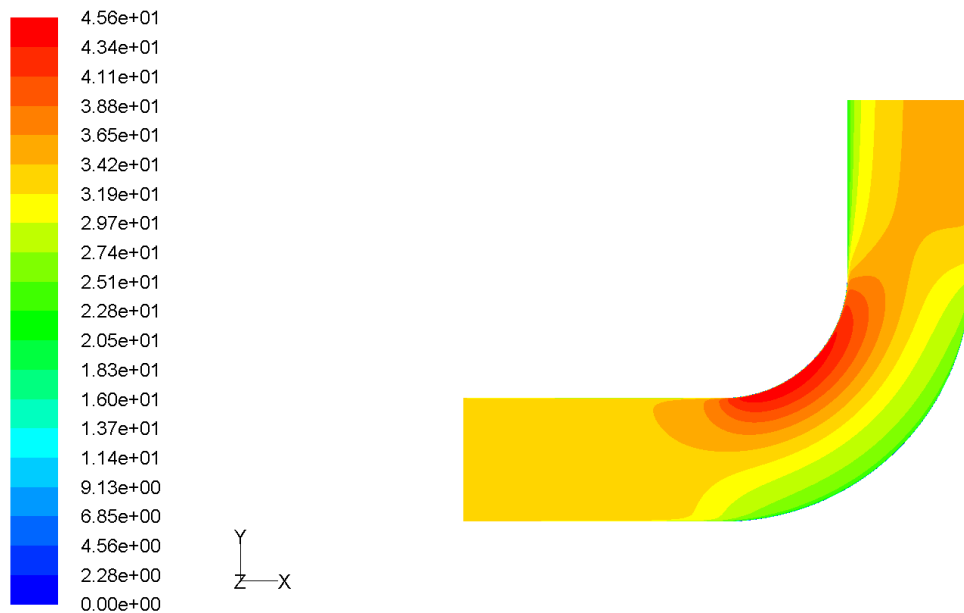
In the next modeling the particulates flow with particles size distribution inside a 90° angled bend with ratio of curve radius to pipe diameter of 1.5 and 56 inches of pipe diameter, was considered based on Lagrangian framework. The particles size distribution is obtained from experimental data (table1) and taken in to account by Rosin-Rammler distribution function. The mass fraction of particles of diameter greater than d is given by Y_d . Table 2 explains the relationship between d and Y_d according to Table1.

The mass flow rate of particles is 0.6 kg/hr which is allocated to particles with different diameters according to their mass fractions. In figure7 the contours of gas velocity are depicted. It is shown that near the inner wall of the bend maximum gas velocity occurs that the radial component of gas velocity leads to dropping particles (especially large one) toward

the outer wall. The trajectory of particles in terms of their diameters, are shown in figure8. The dispersion pattern of solid particles depends on their size and is shown in figure9. As can be seen, the larger particles are moved toward the outer wall of the bend due to radial component of gas velocity. In figure10 the size distribution of particles on different cross sectional planes is drawn versus the relative radial distance according to equation (27). This figure shows that at the outer wall ($r/D=0$), the mean diameter of particles is larger than mean particles diameter at the inner wall ($r/D=1$) which is in consistence with that is mentioned about figure9. We can see from figure10 that at cross sectional plane of 15° there are some small particles near the inner wall of the bend. This plane is located at the region where the radial component of gas velocity starts to increase and still is not reached its final growth. In figure11 the mean particle velocity distribution on each plane is depicted. The variation of particles velocity on each plane is close to a straight line. By increasing the angle of the plane the slope of velocity variation increases. This is because of increasing gas velocity in the vertical section of the bend.

Table 2. The values for d and Y_d

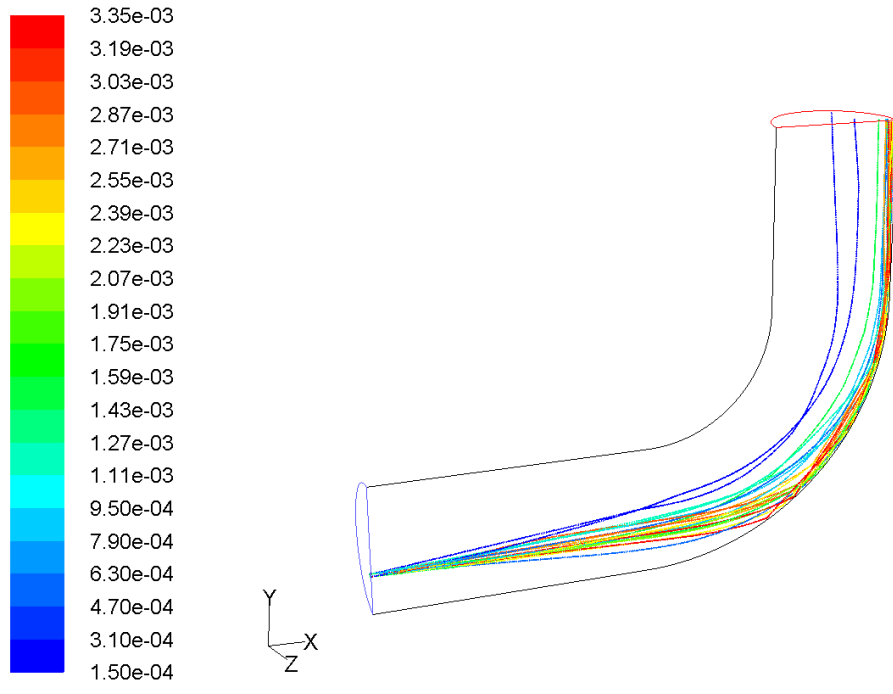
Diameter (μm)	Y_d
150	0.942
212	0.807
300	0.747
425	0.686
600	0.611
850	0.512
1180	0.318
1700	0.226
2360	0.152
3350	0.07



Contours of Velocity Magnitude (m/s) (Time=6.0700e+01)

FILEFN

Figure 7. Contours of gas velocity magnitude



Particle Traces Colored by Particle Diameter (m)

Figure 8. Particles trajectory colored by particle diameter

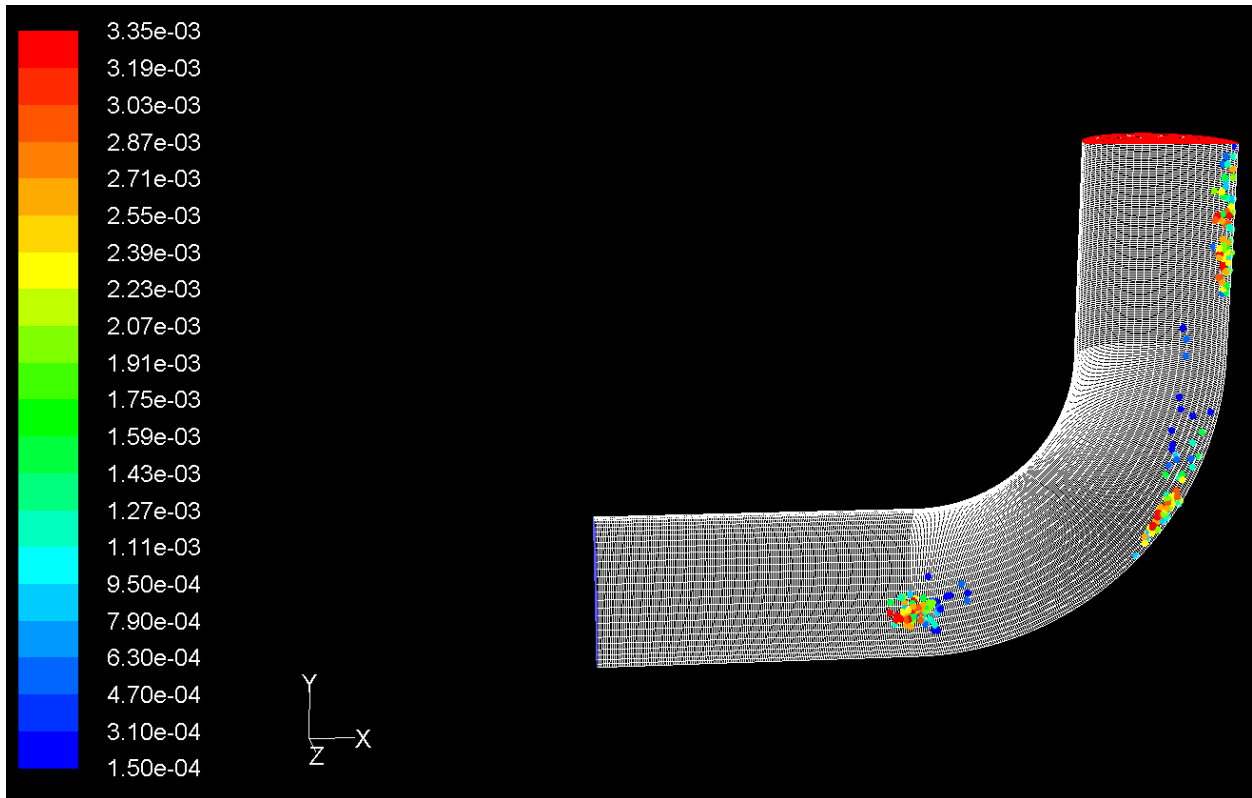


Figure 9. Particles dispersion pattern colored by particle diameter

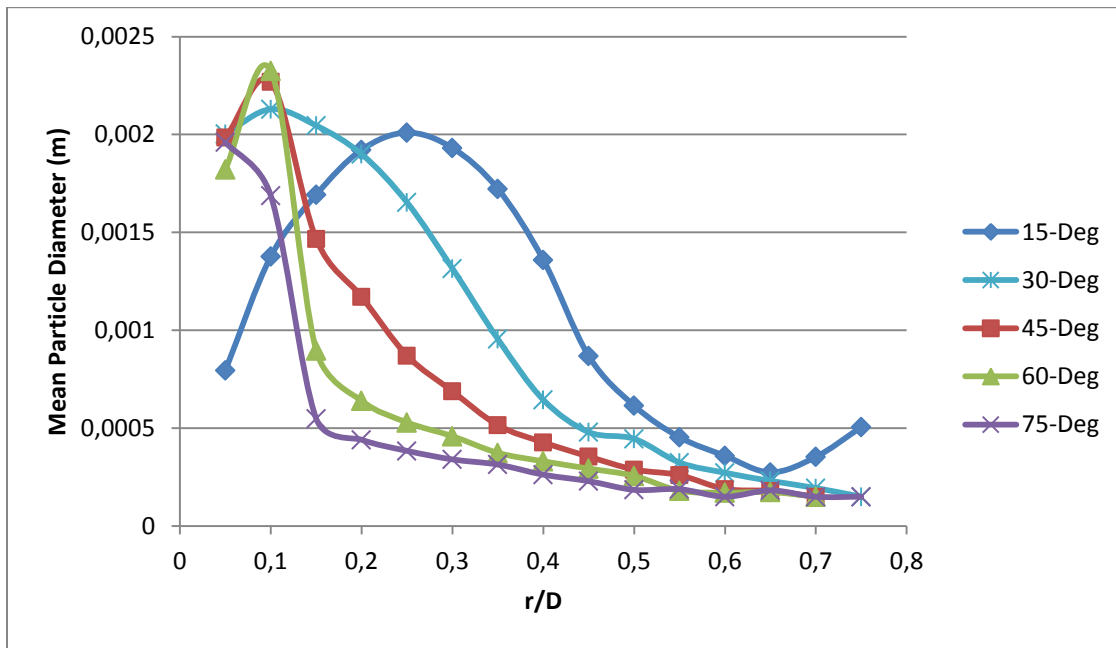


Figure 10. Mean particle diameter distribution on cross sectional planes

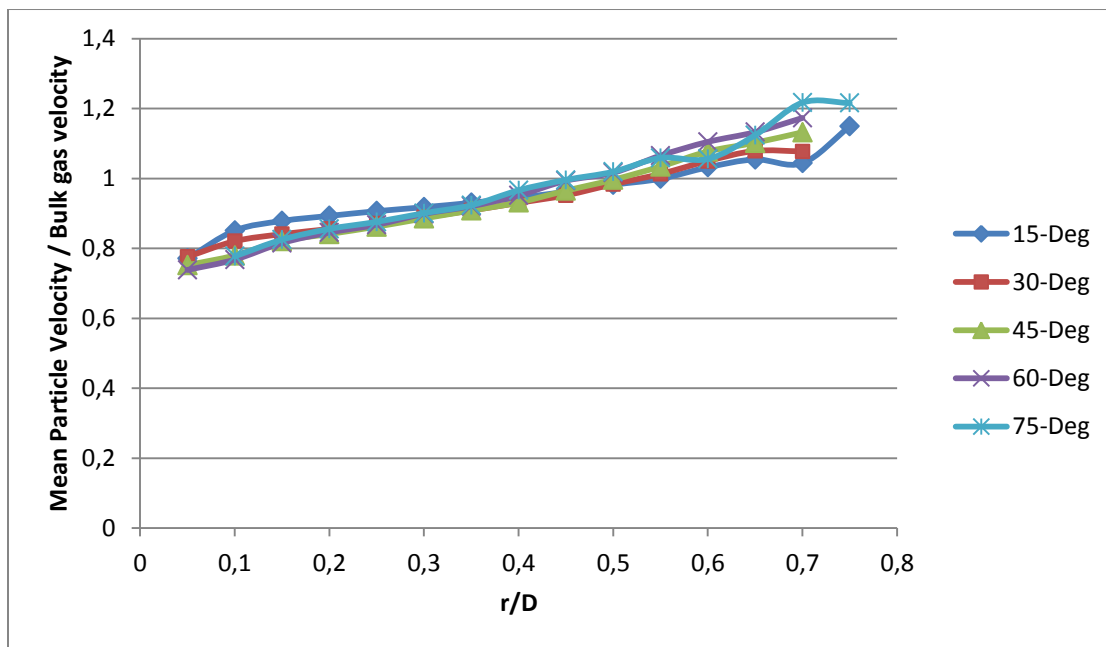


Figure 11. Mean particle velocity distribution on cross sectional planes

7. Conclusion

In this study we have developed a two-phase Eulerian and Lagrangian CFD model to simulate three dimensional particulates motion in gas pipeline. The effect of particles diameter on its fluidization pattern was considered by Rosin-Rammler distribution function. It is shown that for the case of 56 inches pipe diameter, the initial gas rate which is required to fluidize the bed of solid particles is 0.5 m/s and if there is no source of particles inside the pipe there will not any fluidized particle after sufficient elapsed time. Analysis of particulates motion in the bend indicates that due to the increasing trend of radial component of gas velocity through the bend, the larger particles are moved toward the outer wall of the bend and increase the erosion rate at this region. This study proves that we can use CFD modeling as a powerful tool for assessing particulates motion and their erosion effects inside different industrial instruments.

Nomenclature

ρ_k	Phase density (kg.m^{-3})
α_k	Phase volume fraction
U_k	Velocity vector for each phase (m.s^{-1})
τ_k	Stress tensor for each phase (N.m^{-2})
β	Inter phase drag coefficient ($\text{Kg.m}^{-3}.\text{s}^{-1}$)
d	Particle diameter (m)
k_g	Turbulent kinetic energy of gas phase ($\text{m}^2.\text{s}^{-2}$)
ε_g	Turbulent dissipation rate of gas phase ($\text{m}^2.\text{s}^{-2}$)
$\sigma_k, \sigma_\varepsilon$	Turbulent Prandtl number
$G_{k,g}$	Generation of turbulence kinetic energy due to the mean velocity gradients ($\text{Kg.m}^{-1}.\text{s}^{-3}$)
ν	Kinematic viscosity ($\text{m}^2.\text{s}^{-1}$)

References

- [1] Sherik, A.M.: "Black Powder — 1: Study Examines Sources, Makeup in Dry Gas Systems," Oil & Gas Journal, August 11, 2008, Vol. 106, No. 30.
- [2] Sherik, A.M.: "Black Powder — Conclusion: Management Requires Multiple Approaches," Oil & Gas Journal, August 18, 2008, Vol. 106, No. 31.
- [3] Tsochatzidis, N.A.: "Study Addresses Black Powder's Effects on Metering Equipment," Oil & Gas Journal, March 24, 2008, Vol. 106, No. 12.
- [4] Tsochatzidis, N.A. and Maroulis, K.E.: "Methods Help Remove Black Powder from Gas Pipelines," Oil & Gas Journal, March 12, 2007, Vol. 105, No. 10.
- [5] Baldwin, R.M.: "Here are the Procedures for Handling Persistent Black Powder Contamination," Oil & Gas Journal, October 26, 1998, Vol. 96, No. 43.
- [6] Smart, J.: "Determining the Velocity Required to Keep Solids Moving in Liquid Pipelines," paper presented at the Pipeline Pigging and Integrity Management Conference, Houston, Texas, February 14-15, 2007.
- [7] Smart, J. and Winters, R.: "Black Powder Migration in Gas Pipelines and Associated Problems," paper presented at the Pipeline Pigging and Integrity Management Conference, Houston, Texas, February 13-14, 2008.
- [8] Kuan, B. and Schwarz, M.P.: "Numerical Prediction of Diluted Particulate Flows in Horizontal and Vertical Ducts," paper presented at the 3rd International Conference on CFD in the Minerals and Process Industries, CSIRO, Melbourne, Australia, December 10-12, 2003.
- [9] Kuan, B., Yang, W. and Solnordal, C.: "CFD Simulation and Experimental Validation of Diluted Particulate Turbulent Flows in a 90° Duct Bend," paper presented at the 3rd International Conference on CFD in the Minerals and Process Industries, CSIRO, Melbourne, Australia, December 10-12, 2003.
- [10] Kuan, B.: "CFD Simulation of Diluted Gas-solid Two-phase Flow with Different Solid Size Distributions in a Curved 90° Duct Bend," ANZIAM J., 2005, Vol. 46, pp. C744-C763.
- [11] Yang, W. and Kuan, B.: "Experimental Investigation of Diluted Turbulent Particulate Flow Inside a Curved 90° Bend," J. Chemical Engineering Science, 2006, Vol. 61, pp. 3,593-3,601.
- [12] Elsaadawy.E and A. M. Sherik, " Black Powder Erosion in Sales Gas Pipeline Bends", SAUDI ARAMCO JOURNAL OF TECHNOLOGY, FALL 2010.